Supporting Information

All-Polymer Conducting Fibers and 3D Prints via Melt Processing and Templated Polymerization

Anna I. Hofmann,[a]‡ Ida Östergren,[a‡] Youngseok Kim,[b] Sven Fauth,[a] Mariavittoria Craighero,[a] Myung Han Yoon,[b] Anja Lund,[a] Christian Müller[a]**

[a] Department of Chemistry and Chemical Engineering, Chalmers University of Technology, 41296 Göteborg, Sweden

e-mail: hofanna@chalmers.se; christian.muller@chalmers.se

[b] School of Materials Science and Engineering, Gwangju Institute of Science and Technology, Gwangju 61005, Republic of Korea

‡These authors contributed equally.

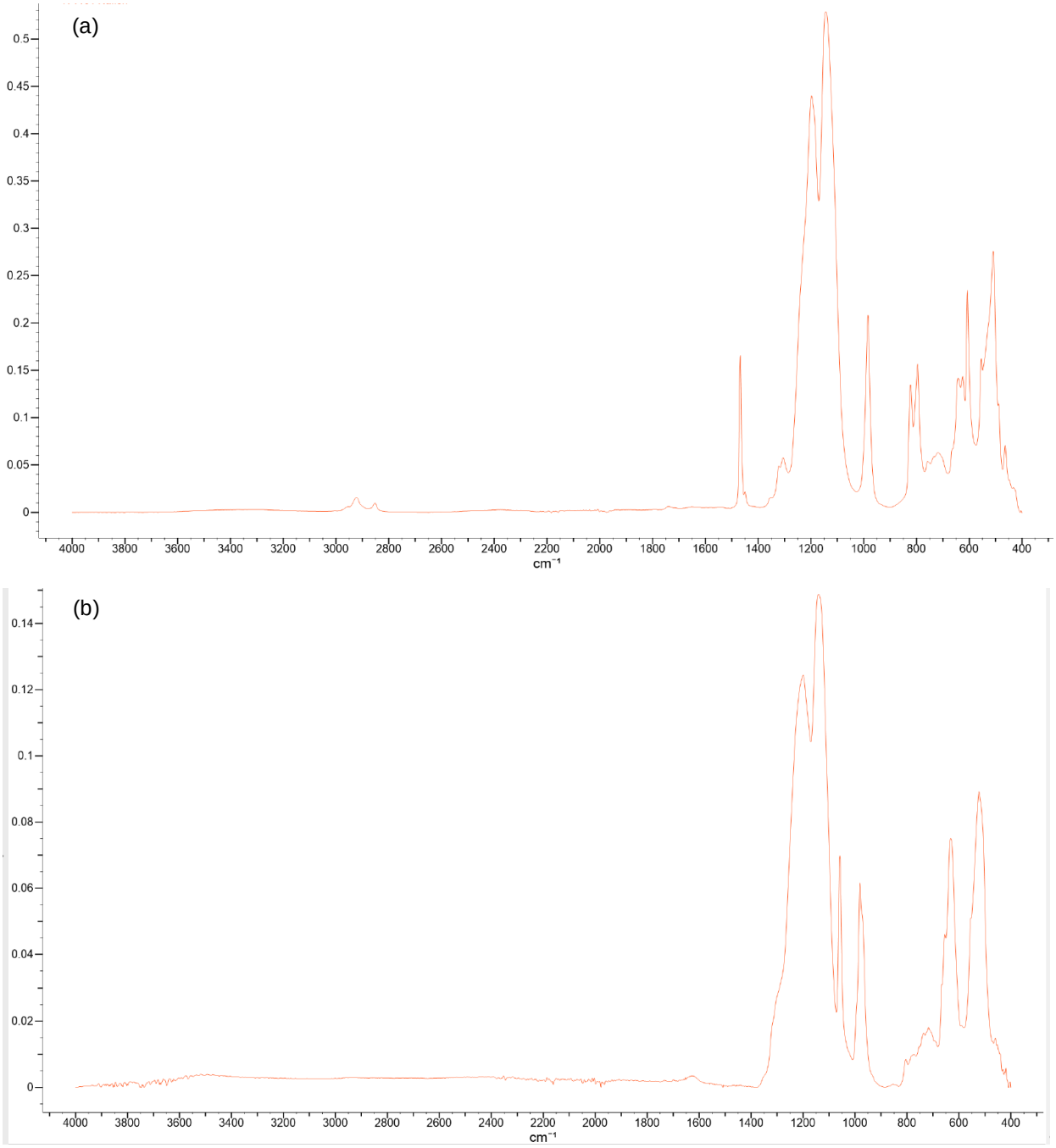

Figure S1. FTIR spectra of (a) the Nafion precursor and (b) the activated Nafion. The decrease of the band at ca. 1470 nm^{-1} (asymmetric stretching of O=S=O in $-SO_2F$) and the increase of the band at around 1050 nm^{-1} (asymmetric stretching of O=S=O in $-SO_3$) confirms the transformation of the sulfonyl fluoride groups into sulfonic acid groups.

sample		C	H	S	O	F	K
Activated Nafion	experimental	20.9	0.7	2.9	10.5	61.0	3.8
	theoretical	20.1	0.6	3.0	11.1	61.7	3.6
PEDOT:Nafion	experimental	23.5	0.7	8.5	14.1	51.8	-
	theoretical	23.8	0.6	8.1	14.3	51.7	-

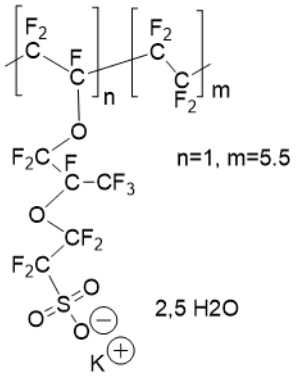

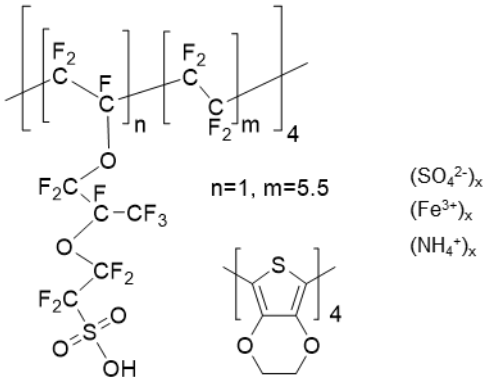

Table S1. Composition in wt% of melt processed, activated Nafion and PEDOT:Nafion. The theoretical composition was determined by calculating the composition of hypothetical PEDOT:Nafion complexes with different PEDOT to Nafion ratios and matching the results with the experimental values. The chemical structures represent the structures that match the theoretical composition listed in the table.

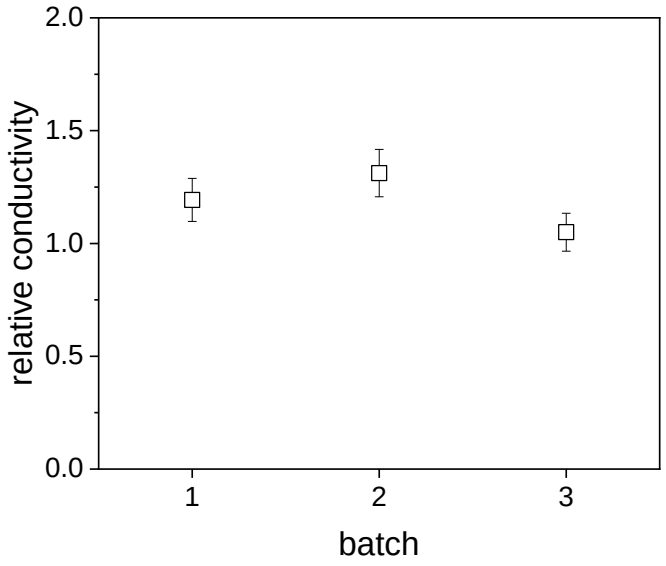

Figure S2. Relative conductivity of three different batches PEDOT:Nafion after one year storage under ambient conditions with respect to the initial conductivity, measured right after synthesis. Every measurement point represents the average of three values, measured on different positions of a PEDOT:Nafion filament from the same respective batch.

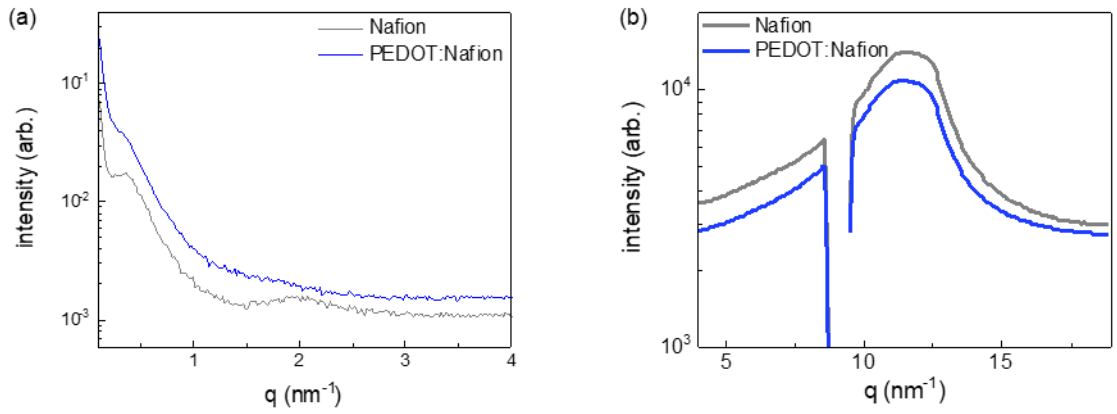

Figure S3. (a) SAXS and (b) WAXS diffractograms of melt processed activated Nafion (gray line) and PEDOT:Nafion (blue line).

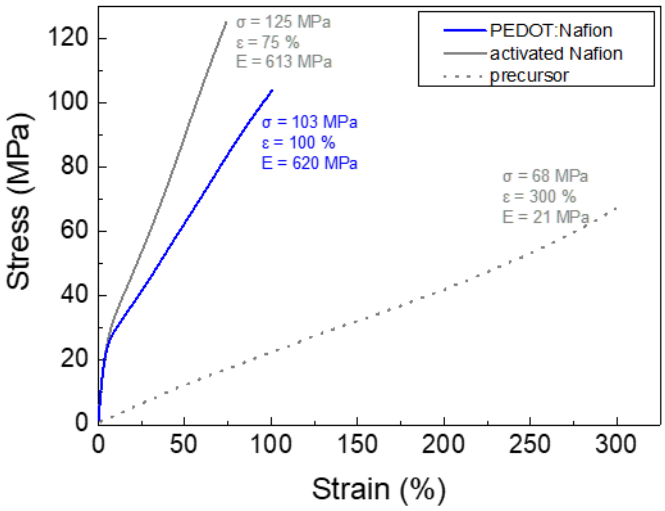

Figure S4. Mechanical properties of melt spun fibers of the Nafion precursor, activated Nafion and of PEDOT:Nafion measured by tensile testing.

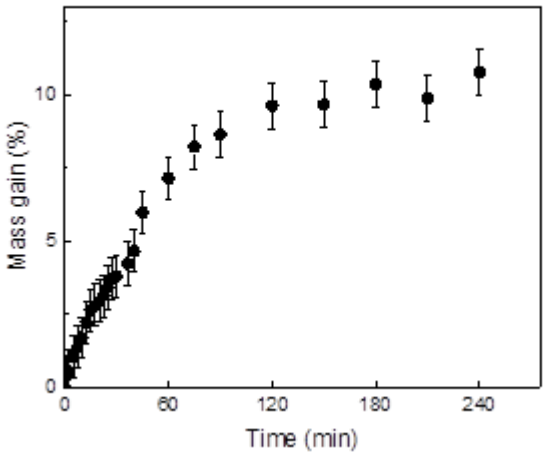

Figure S5. Mass gain of bulk PEDOT:Nafion placed in a water bath over time.

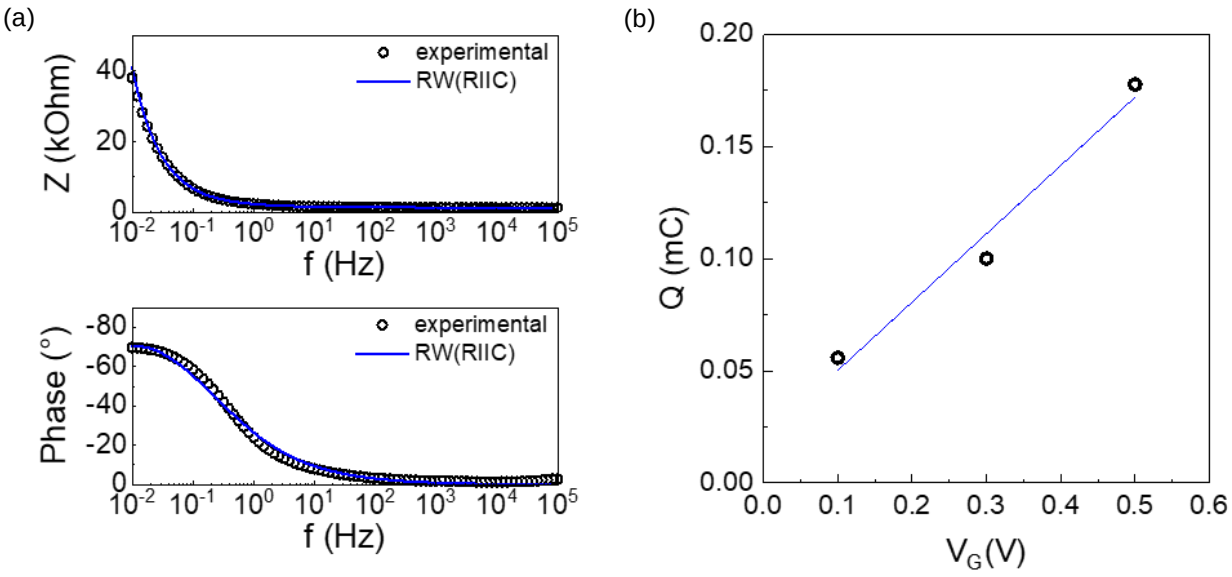

Figure S6. (a) Impedance spectroscopy of a PEDOT:Nafion fiber (L=1.9mm, d=150 µm,V= 3.4*10^{-5} cm^3), fitted with a R_sW(R_pIIC) equivalent circuit, R_s=1395 Ohm, W=0.00037, R_p= 2*10^5 Ohm, C = 0.0005 F, C*= 14.7 Fcm^{-3}. (b) Gate current transient of a PEDOT:Nafion fiber (L=2mm, d=0.2mm), the fitted line corresponds to C = 0.0003 F (x-intercept = -0.065 V, R^2 = 0.98), C*= 8.8 Fcm^{-3}.

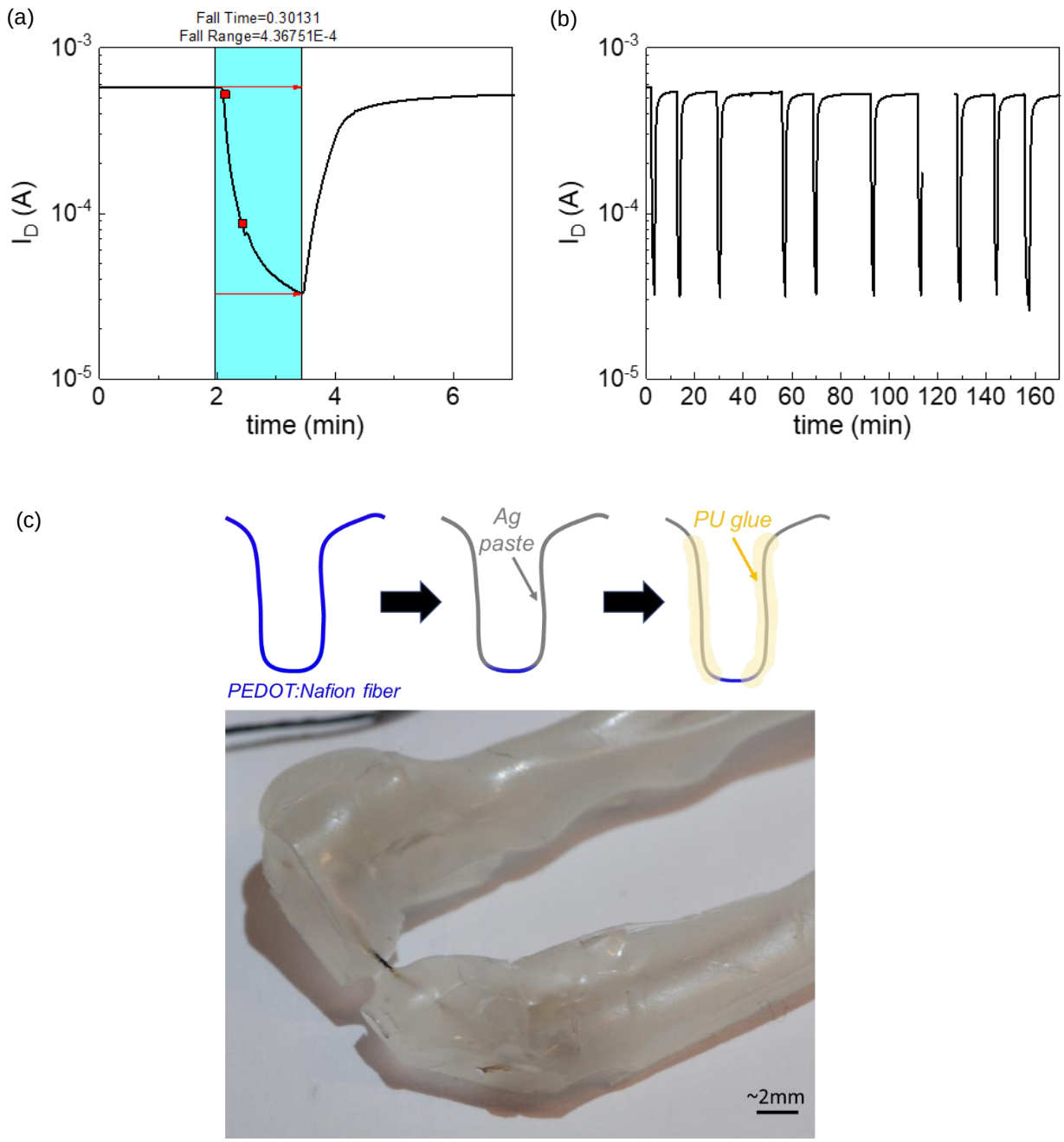

Figure S7. Time response of the drain current of a PEDOT:Nafion fiber OECT for a gate voltage pulse of 0.6 V (a) for one cycle and (b) over 10 cycles. (c) Schematic and photograph of a PEDOT:Nafion fiber OECT.

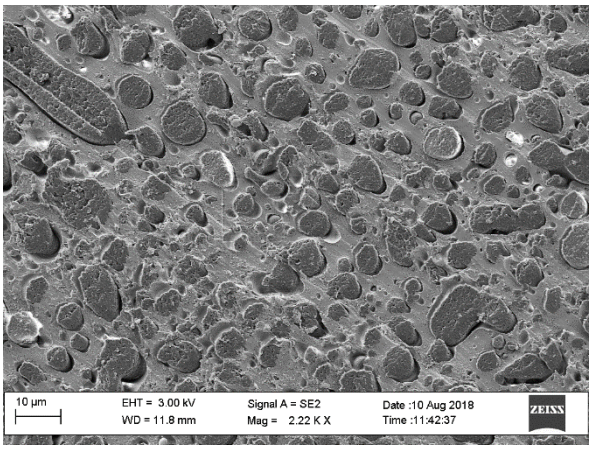

Figure S8. Scanning electron micrograph of a Nafion/ABS blend containing 30 wt% ABS.

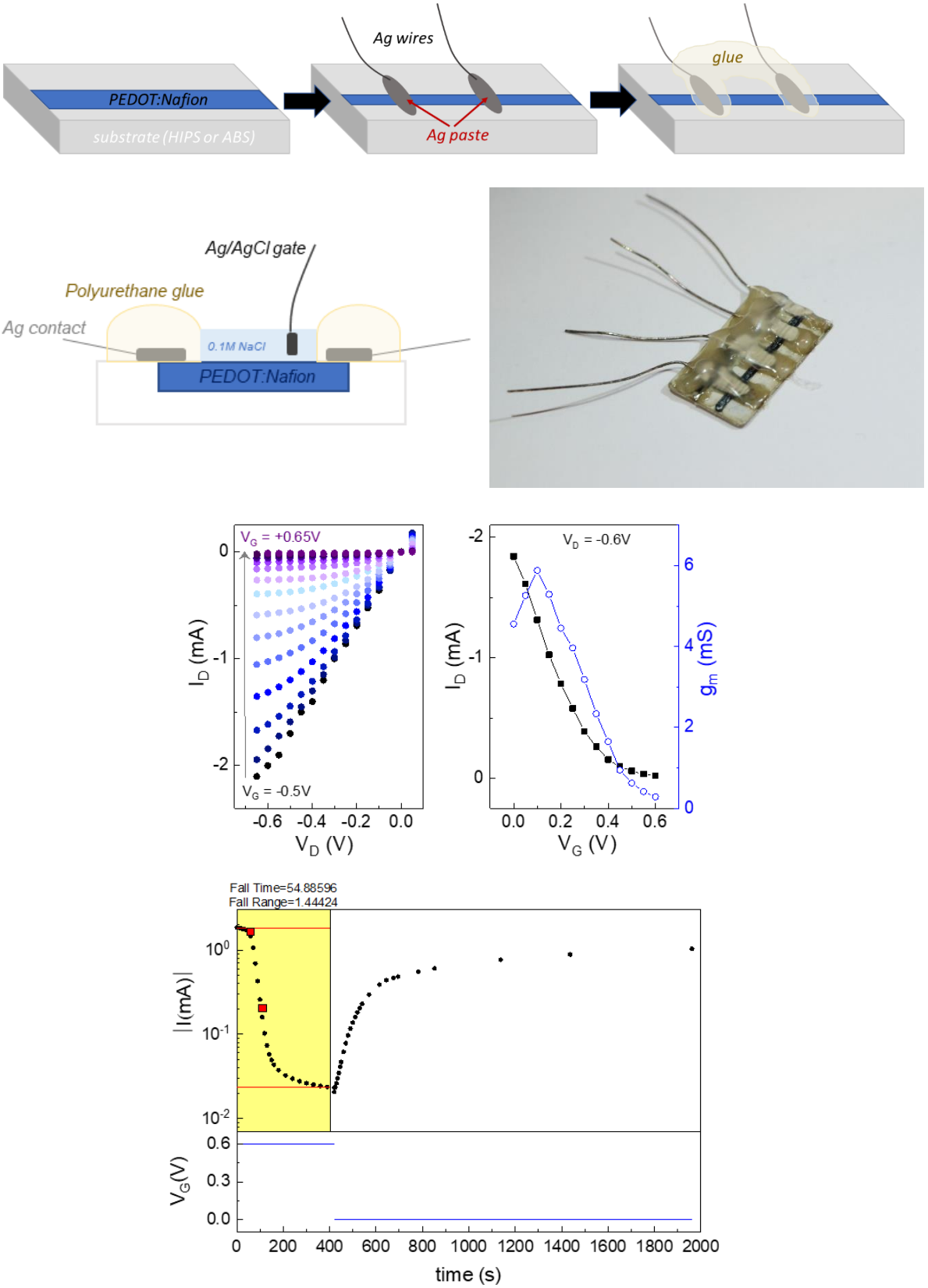

Figure S9. OECT design scheme, photograph, output characteristics and time response of a 3D printed PEDOT:Nafion line (L=1.5 mm, d=30 µm, W=1 mm).